

PACS numbers: 42.55.Lt; 42.60.Lh; 52.80.–s
DOI: 10.1070/QE2012v042n06ABEH014631

Pulsed hollow-cathode ion lasers: pumping and lasing parameters

S.P. Zinchenko, I.G. Ivanov

Abstract. **Optimal discharge conditions have been experimentally found for ion lasers excited in the hollow-cathode discharge plasma by microsecond current pulses by pumping working atoms in second-kind collisions with ions and metastable buffer-gas atoms. Measurements of the output power of krypton ion and zinc-, cadmium-, mercury-, thallium-, copper-, and gallium-vapour lasers in tubes with cathodes of different diameters showed that the pulse power reaches several tens of watts, and the average power obtained with cathodes 2 cm in diameter and a length of 40 cm or more approaches 1 W. Lasing in most media is observed simultaneously at several lines (the multi-wavelength regime). Lasing on a three-component (He–Kr–Hg) mixture is realised in the multi-wavelength regime at blue, red, and IR lines.**

Keywords: *ion laser, pumping by second-kind collisions, hollow-cathode discharge, multi-wavelength laser.*

1. Introduction

Ion metal-vapour and gas lasers are known by the ability to emit in the short-wavelength region of the spectrum (visible, etc.) as well to generate simultaneously at several laser lines. Apart from the conventional method of pumping ionic transitions in gas lasers in a positive-column (PC) plasma of a longitudinal discharge, for the transitions which are excited by second-kind collision with buffer-gas atoms there exists a more efficient method of pumping: in the negative-glow (NG) region of an abnormal glow hollow-cathode discharge (HCD). The advantages of this type of discharge over the longitudinal discharge are discussed in [1, 2].

Because in the HCD there can form spatial inhomogeneities associated with the transition from a glow discharge to the arc discharge, in the stationary and quasi-stationary regimes it was impossible to implement the optimal pump power. As a result, the lasing power on the lines did not reach maximum values. Earlier we have shown [3] that when the HCD is excited by short current pulses of microsecond duration (0.1–10 μs), it is possible avoid the development of inhomogeneities in the discharge plasma, and consequently raise the level of pumping of the active medium. In addition, changing the pulse repetition rate it is possible to adjust the mean value of the deposited pump power and laser power. In [4, 5], we have carried out theoretical studies of the kinetics of the active media of metal-vapour hollow-cathode lasers with charge-exchange pumping, which allowed us to explain the temporal behaviour of the inversion for known and new ion laser transitions of metals. However, at present a detailed study of the energy characteristics of pulsed ion hollow-cathode lasers has not yet been completed.

In the present paper, for a large group of the most effective hollow-cathode lasers on the ion transitions in Zn, Cd, Hg, Tl, Cu, Ga and Kr by optimising the discharge conditions, namely the cathode-cavity geometry, the concentration of working atoms and atoms of the buffer inert gas (He, Ne), as well as the amplitude, duration and pulse repetition rate current, we have experimentally determined limiting energy characteristics of lasers – the average and peak (pulsed) output power. As a result, we have obtained output powers, much higher than the corresponding values in the cw and quasi-cw regimes.

2. Mechanisms of inversion formation and optimal density of working atoms and buffer-gas atoms

Pumping of ion quantum states of metals and heavy noble gases in the mixtures with a light buffer inert gas in the NG HCD region of the active medium in lasers under consideration is realised due to inelastic second-kind collisions of metal atoms with buffer-gas ions (charge exchange)

$$M_0 + B_0^+ \rightarrow M^{+*} + B_0 + \Delta E(\infty), \tag{1a}$$

where M_0 and M^{+*} are an atom in the ground state and an excited metal ion; B_0 and B_0^+ are an atom and a buffer-gas ion in the ground state; $\Delta E(\infty)$ is the energy difference between the ions in the B_0^+ and M^{+*} states. Pumping is also due to inelastic second-kind collisions of metal atoms or ions of heavy inert gas with metastable buffer-gas atoms (Penning ionisation and resonant excitation transfer, respectively):

$$M_0 + B_m \rightarrow M^{+*} + B_0 + e + \Delta E(\infty). \tag{1b}$$

$$A_0^+ + B_m \rightarrow A^{+*} + B_0 + \Delta E(\infty), \tag{1c}$$

where B_m is an excited (metastable) buffer-gas atom; A_0 and A^{+*} is the ion of heavy inert gas (Kr, etc.) in the ground and excited states. Reactions (1a) and (1c) are 'resonant' with $\Delta E(\infty) \sim kT$, reaction (1b) can occur at any $\Delta E(\infty) > 0$, since the excess energy ΔE in the separation of the heavy particles is carried away by the electron.

S.P. Zinchenko Southern Scientific Center, Russian Academy of Sciences, ul. Chekhova 41, 344006 Rostov-on-Don, Russia;
I.G. Ivanov Department of Physics , Southern Federal University, ul. Zorge 5, 344090 Rostov-on-Don, Russia; e-mail: ig.ivanov@mail.ru

Received 20 April 2011; revision received 21 February 2012
Kvantovaya Elektronika **42** (6) 518–523 (2012)
Translated by Yu.P. Sin'kov

The properties of the NG HCD plasma provide its advantages over PC plasma while pumping M^{+*} and A^{+*} levels in reactions (1), the main one being the presence of an excess of both fast and thermal electrons in the electron energy distribution in the NG HCD (compared with a Maxwellian distribution in the PC) [6]. The group of fast electrons acquires in the cathode fall (CF) region of a potential U_{cf} an energy $\varepsilon_0 \approx eU_{cf}$ (for example, in the pulsed HCD $\varepsilon_0 \leqslant 2$ keV) and performs in the NG a predominantly effective ionisation and excitation of a buffer inert gas [creates energy donors B_0^+ and B_m for the reactions (1)]. The group of thermal electrons with average energy $kT_e \sim 1$ eV as a result of the effective superelastic collisions redistributes the ions M^{+*} and A^{+*} in closely spaced quantum levels [3–5, 7].

The partial cross section for the charge exchange $Q^i_{\text{ch-tr}} = \xi_i Q_{\text{ch-tr}}$ (1a) on the ith level of the ion M^{+*} is determined by the partial charge-exchange ratio ξ_i – the probability of population of the ith level ($\xi_i \leqslant 1$ and $\sum_i \xi_i = 1$; $Q_{\text{ch-tr}}$ is the total cross section for the charge exchange on all levels M^{+*}). The rate of population of the ith excited level of the metal ion $M^{+*}(i)$ in the processes of charge exchange is

$$W^i_{\text{ch-tr}} = N(B_0^+)\, N(M_0)\, K^i_{\text{ch-tr}} = \xi_i W_{\text{ch-tr}}$$

$$= \frac{W(B_0^+)\, N(M_0)\, \xi_i K_{\text{ch-tr}}}{\nu(B_0^+) + N(M_0) K_{\text{ch-tr}}}. \qquad (2)$$

Here N is the particle concentration; $K^i_{\text{ch-tr}} = \overline{VQ^i_{\text{ch-tr}}} = \xi_i \overline{VQ_{\text{ch-tr}}} = \xi_i K_{\text{ch-tr}}$ is the ith level population constant, i.e., the partial charge-exchange cross section $Q^i_{\text{ch-tr}}$, averaged over relative velocities V of colliding particles; $K_{\text{ch-tr}}$ is the total charge-exchange rate to all levels M^{+*}; $W(B_0^+)$ is the buffer-gas ionisation rate; $\nu(B_0^+)$ is the total frequency of deactivation of B_0^+ ions due to the ambipolar diffusion and recombination; and $N(M_0)K_{\text{ch-tr}}$ is the total frequency of deactivation of these ions during the charge-exchange processes.

The maximum pumping rate meets the optimal concentration of working atoms $N(M_0)^{\text{opt}}$, when B_0^+ ions are predominantly deactivated in charge-exchange reaction and the number of fast electrons producing B_0^+, is still large, i.e., when

$$N(M_0)\, K_{\text{ch-tr}} \geqslant \nu(B_0^+). \qquad (3)$$

In this case, from (2) we have

$$W^i_{\text{ch-tr}} \approx \xi_i W(B_0^+),$$
$$W_{\text{ch-tr}} \approx W(B_0^+), \qquad (4)$$

i.e., at $N(M_0)^{\text{opt}}$ the total rate of pumping all levels M^{+*} in the NG HCD in the charge-exchange processes is $W(B_0^+)$. For example, the optimal concentrations for the He–Hg and Ne–Tl mixtures are as follows: $N(Hg_0)^{\text{opt}} \geqslant 2.5\times10^{15}$ cm^{-3} and $N(Tl_0)^{\text{opt}} \geqslant 4\times10^{15}$ cm^{-3}.

In the case of pumping the M^{+*} levels as a result of Penning ionisation (1b) or the A^{+*} levels at the resonant excitation transfer (1c), the relations similar to (2)–(4) are also valid.

In the HCD with a cathode cavity of cylindrical shape at an optimal concentration of metal vapours the dependence of $W(B_0^+)$ on the buffer gas pressure is determined by two factors: the decrease in the number of fast electrons in the radial direction on their way from the boundary of the CF–NG zone (near the wall of the cathode cavity) to the NG axis through the inelastic ionising collisions, as well as the concentration of electrons as a result of their 'focusing' in the axial zone. If at the boundary of the CF–NG zone the initial electron energy $\varepsilon_0 \approx eU_{cf}$, then for the effective cross section of ionisation of the gas q_i and the average energy lost by an electron due to ionisation, $\sim 2\varepsilon_i$ (ε_i is the ionisation potential of the gas), the criterion for the optimal gas concentration $N(B)^{\text{opt}}$ can be derived from the fact that the total length of the fast electron path λ must be equal to the radius of the cathode cavity $R_{\text{cat}} = d_{\text{cat}}/2$, i.e.,

$$\lambda \approx \frac{eU_{cf}}{2q_i\varepsilon_i N(B)^{\text{opt}}} \approx \frac{d_{\text{cat}}}{2}. \qquad (5)$$

For the investigated mixtures pumped in the charge-exchange processes in the HCD at the current pulse duration of 0.5–1 μs and $U_{cf} \approx 2\times10^3$ V, the similarity relations, which can be found from (5), are as follows: $N(He)^{\text{opt}} d_{\text{cat}} \approx 10^{18}$ cm^{-2} and $N(Ne)^{\text{opt}} d_{\text{cat}} \approx 9\times10^{17}$ cm^{-2}. Similarly, the criterion can be obtained for reactions (1b) and (1c).

3. Optimal discharge current

When feeding the HCD by microsecond current pulses, the instant when the discharge uniformity is broken (i.e., arc arises) shifts to higher currents (unlike the quasi-steady-state regime), because inhomogeneities cannot develop for several (or several tenths) microseconds; therefore, using a pulsed HCD, one can easily obtain cathode-surface current densities on the order of several A cm^{-2}, which are several orders of magnitude higher than those typical of the steady-state regime. In addition, it turned out that the U_{cf} value increases with a decrease in the pulse duration and exceeds several times the U_{cf} value in a steady-state discharge at a current pulse duration of ~1 μs. Correspondingly, the energy ε_0 of monoenergetic electrons and the pumping rate in reactions (1) also increase. An increase in the accelerating voltage rises also the relative number of these electrons [8]. As compared with a steady-state HCD, this circumstance allows one to increase the cathode-cavity diameter (i.e., the active-medium volume) without deteriorating the lasing efficiency. This rise is accompanied by an additional increase in U_{cf} and ε_0.

To create an active medium of lasers, we used discharge tubes, as shown in Fig. 1. The studied substances (Zn, Cd, Hg, Tl, Cu, Ga, and Kr) do not chemically interact with the tube electrodes and are potentially suitable for lasing at several wavelengths while pumped by second-kind collisions; the vapour pressure of 10–50 Pa (optical for the HCD), which allows one to achieve the complete transfer of excitation from the buffer gas during second-kind collisions [see (3), (4)], is easily produced by thermal evaporation at moderate temperatures [1, 2]. The current pulse was formed by a complete discharge of the storage LC-line through the discharge gap and thyratron-switch, or by a partial discharge through a beam tetrode.

4. Low pulse repetition rate

The experiment showed that, at a current pulse repetition rate f up to several kHz and optimal current value, the pulse power for all storage lines under study was independent of the frequency. Table 1 contains the values of unsaturated gain and specific pulse power for the strongest transitions in the Zn, Cd, Hg, Tl, Cu, Ga, and Kr spectra under optimal excitation conditions and $f = 1$ kHz.

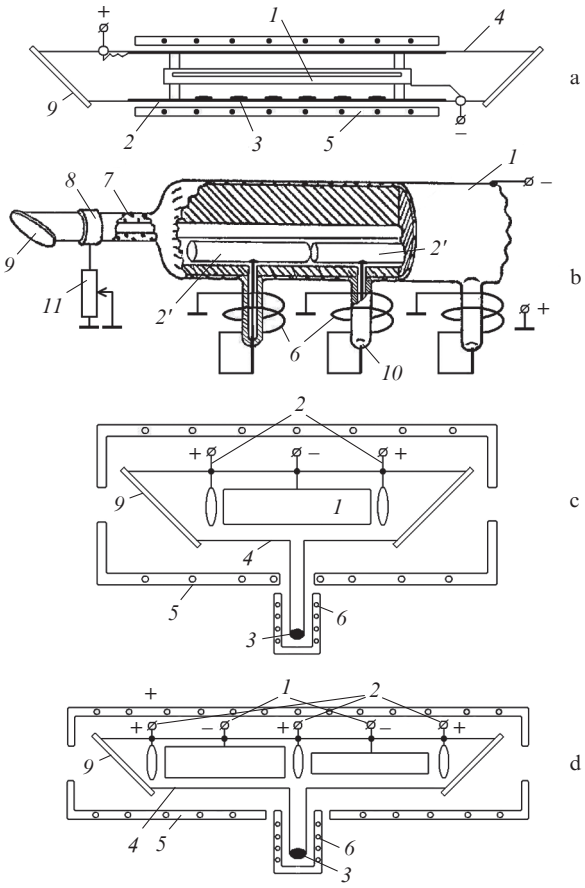

Figure 1. Schematic diagrams of discharge tubes of HCD lasers excited by microsecond current pulses of (a, b) transverse and (c, d) longitudinal–transverse types (panel d shows a tube with cathodes of different diameters for measuring specific radiation power): (*1*) cathode (see cathode unit in panel b); (*2*) anodes [(*2′*) anode units]; (*3*) working material; (*4*) tube vacuum envelope (glass, quartz, or ceramics); (*5*) thermostat (tube heater); (*6*) evaporator heater; (*7*) terminal blocking cataphoresis section with an additional anode (*8*); (*9*) Brewster window; (*10*) evaporator; (*11*) ballast of blocking unit.

Note that, for a given material, lasing occurred both at each laser line taken separately and simultaneously at all lines, i.e., in the multi-wavelength regime. The best characteristics were observed for the helium–mercury-vapour, helium–copper-vapour and neon–thallium-vapour lasers with charge-exchange pumping (1a), and the helium–cadmium-vapour and helium–krypton-vapour lasers operating in the short-wavelength part of the spectrum (1b) and (1c). The comparison shows that the power in the case of microsecond pumping is substantially higher than that in the quasi-cw excitation regimes. For example, for 615-nm lines of the Hg^+ ion and 780.8-nm lines of the Cu^+ ion the specific power is $P_p^{spec} = 0.5$ and 0.4 W cm^{-3}, respectively, compared with 0.023 [9] and 0.01 W cm^{-3} [10] in the quasi-cw regime.

Figure 2 shows the typical time characteristics of helium–mercury-vapour laser and the dependences of some laser parameters on the current pulse duration τ. The power saturation is caused by accumulation of thermal electrons in the NG HCD plasma and by the inclusion of the redistribution of M^{+*} ions over the levels due to de-exciting collisions with them [3]. Measurements showed that for any τ in the case of a tube with a cathode of larger diameter (4 cm) the maximum total output power and efficiency are achieved.

Table 1. Characteristics of HCD lasers at optical concentrations of the active-medium components and a low f (f = 1 kHz, τ = 1 μs, slit cathode with a cavity diameter d_{cath} = 0.6 cm).

Particle	Wavelength/nm	Buffer gas, pumping mechanism	Discharge current density/A cm^{-2}	Unsaturated gain/dB m^{-1}	Specific radiation power/W cm^{-3}
Zn II	491.2	He (CE)	0.43	7	0.15
	492.4		0.43	7.5	0.15
	610.2		0.22	2	–
	758.8		0.28	5	0.017
	589.4	He (PI)	0.54	3.5	–
	747.9			5	–
Cd II	441.6	He (PI)	0.20	5	0.25
	533.7	He (CE)	0.15	4.5	0.04
	537.8		0.15	4.5	0.04
	636.0		0.095	2.5	–
	728.4		0.15	6	–
	806.7		0.15	7.5	–
Hg II	615.0	He (CE)	0.9	39	> 0.50
	794.5		0.6	35	–
Tl II*	595.0	Ne (CE)	0.34	15	0.47
	695.0		0.15	9	0.10
	707.0		0.1	3.8	0.05
Cu II	780.8	He (CE)	~1,0	33,5	0,40
Ga II	633.4	Ne (CE)	0.6	13	–
	719.8			10.7	–
Kr II	431.8	He (RET)	1.5	< 2	
	469.4			6	~0.50

Note: CE, PI, and RET denote, respectively, charge exchange, Penning ionisation, and resonant excitation transfer;; *d_{cat} = 0.9 cm.

5. High pulse repetition rate

The pulse and average output powers in the repetitively pulsed regime were measured at $f \leqslant 10$ KHz and $\tau = 0.3–1$ μs. In the ranges from 0 to 5 kHz for mercury- and thallium-vapour lasers and from 0 to 2 kHz for cadmium-vapour lasers, the pulse power P_p was maximum and independent of f, while the average power P_{av} linearly rose with an increase in the pulse repetition rate. With a further increase in the pulse repetition rate, P_p began to decrease, and the P_{av} value became saturated at the optimal f, with subsequent reduction (Fig. 3).

The measurements at f = 10–100 kHz were carried out upon HCD excitation by trains of pulses, from two (dual-pulse method) to 75 pulses per train, at $\tau = 0.3–1.0$ μs (Fig. 4). It was found that incomplete decay of plasma and accumulation of thermal electrons occur over the time between two subsequent pulses; i.e., a residual conductivity exists in the cathode cavity at the arrival of each subsequent pulse, as a result of which the discharge voltage $U \approx U_{cf}$ decreases (Fig. 4b). The accumulation of electrons enhances the electronic relaxation of levels [3], and the decrease in U_{cf} leads to a decrease in the formation rate of B_0^+ and B_m in NG due to the decrease in the primary-electron energy [8].

Table 2 presents the optimal f values (corresponding to maximum P_{av}) for different τ and d_{cath} values and P_p and P_{av}

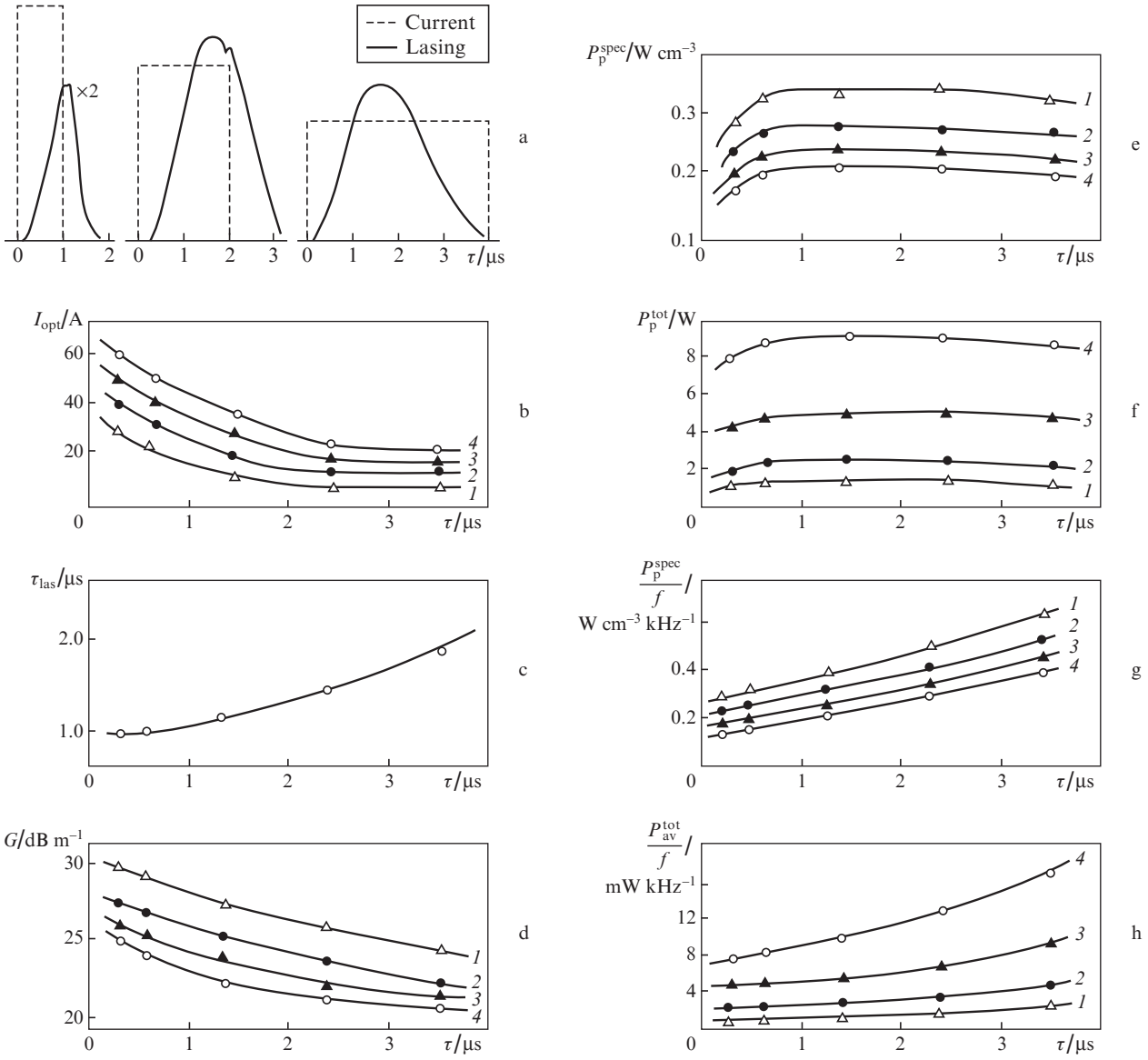

Figure 2. (a) Oscillograms of the current and lasing pulses and (b–h) the dependences of (b) the optimal pump current, (c) the lasing pulse duration, (d) the gain, (e) the specific pulse power, (f) the total pulse power, (g) the specific average power, and (h) the total average power on the pump current pulse duration; 615-nm HgII laser line; cathodes with diameters of (*1*) 0.6, (*2*) 0.9, (*3*) 1.4, and (*4*) 2.0 cm; helium pressure is 1.1 kPa.

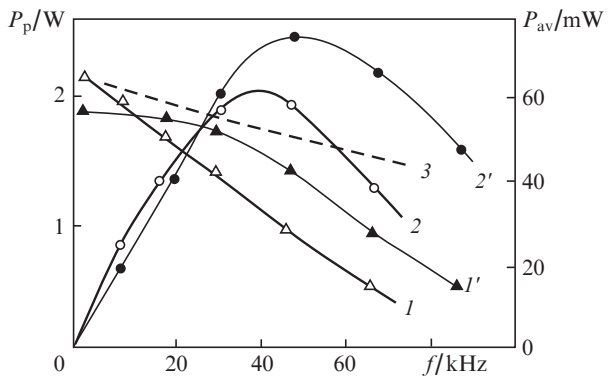

Figure 3. Dependences of the (*1*,*1'*) pulsed and (*2*,*2'*) average radiation power at the 615-nm HgII line on the pulse repetition rate at current pulse durations of (*1*,*2*) 1 and (*1'*,*2'*) 0.3 μs (the cathode diameter is 0.9 cm) Curve (*3*) is the result of calcualtions.

values for these repetition rates, as well as the powers at low f in the repetitively pulsed regime. One can see that if at low repetition rates and τ = 1 μs the average power (Fig. 2) is higher than at τ = 0.3 μs, whereas at f > 20 kHz the pattern changes: higher P_{av} corresponds to shorter τ, which is determined by the less sharp decrease in P_p in this case. In other words, at high (including optimal) f, shorter current pulses are preferred. Note that the curves presented in Fig. 3 behave similarly for cathodes of all diameters under consideration. A lower optimal pulse repetition rate for the Ne–Tl, He–Cd, and He–Kr lasers is determined by the fact that in this case the pulse power decreases faster with increasing f.

At high repetition rates and low krypton and metal-vapour pressures (from 2 to 5 Pa) N(M) somewhat decreases in the paraxial tube regions, which is caused by the cataphoresis separation of the gas mixture in pulsed HCD NG, where an electric field $E \sim 10^2$ V cm^{-1} acts in the direction from the axis of the cathode to its wall. This effect flattens out the radial profile of the laser line intensities [6].

Table 2. Characteristics of He–Cd, He–Hg, Ne–Tl, and He–Kr HCD lasers at high pulse repetition rates.

Particle	Wavelength/nm	d_{cat}/cm (cathode cavity length/cm)	τ/μs	I_p/A	f/kHz	P_p/W (P_p^{spec}/W cm^{-3})	P_{av}/mW (P_{av}^{spec}/mW cm^{-3})
Cd II	441.6	0.9 (40)	1.0	20	13[1]	3.5 (0.14)[2]	46 (1.8)
	533.7 537.8	0.9 (40)	1.0	15	13[1]	0.5 (0.02)	6.5 (0.26)
Hg II	615.0	0.9 (40)	1.0	105	41[1]	5.9 (0.24)	290 (11.6)[3]
			0.3	125	50[1]	6.3 (0.26)	310 (12.4)[3]
		2.0 (40)	1.0	180	10	32 (0.25)	380 (2.6)[4]
				205	34[1]	15 (0.12)	610 (5.1)[3]
			0.3	215	10	29 (0.23)	290 (2.1)[4]
				250	40[1]	24 (0.2)	880 (7.04)[3]
		2.0 (100)	0.3	650	10	72 (0.23)	720 (2.1)[4]
		4.0 (40)	1.0	290	28[1]	29 (0.06)	970 (2.5)[3]
			0.3	320	31[1]	42 (0.084)	1300 (2.0)[3]
Tl II	595.0	0.9 (40)	1.0	40	10	10 (0.23)	130 (5.1)[4]
				45	22[1]	5.2 (0.2)	160 (6.4)[3]
		1.45 (40)	0.5	70	18[1]	9.8 (0.14)	195 (3)[3]
		2.0 (40)	1.0	150	15[1]	13.5 (0.11)	285 (2.3)[3]
Kr II	469.4	0.8 (40)	0.5	140	1 15[1]	~10 (0.5) ~5 (0.25)	12.5 (0.62) 90 (4.5)[1]

[1] – optimal f; [2] – up to 250 mW cm^{-3} at a low f for a cathode 0.6 cm in diameter; [3] – excitation by pulse trains, $\Delta T \approx 4$ ms; [4] – repetitively pulse regime, f is below optimal.

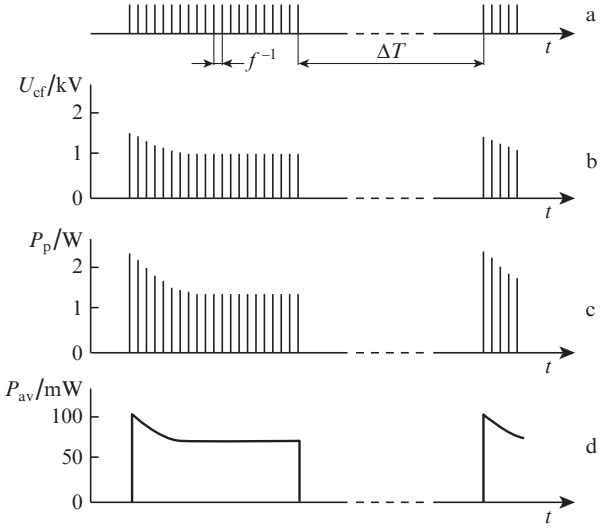

Figure 4. Oscillograms of (a) the current pulse trains, (b) the voltage across the tube $U \approx U_{cf}$, and the (c) pulsed and (d) average radiation powers at the 615-nm Hg II line (cathode diameter 0.9 cm, $f = 40$ kHz, $\tau = 1$ μs).

6. Multi-wavelength lasing in a mixture of several working materials

Because the processes of direct ionisation predominate over the step ones in the NG HCD, by placing several working materials (active media) in one HCD tube it is reasonable to select them in such a way as to prevent the energy of each buffer-gas donor particle (B_0^+ or B_m) from redistribution between the active particles of different types and to 'pump' particles of only one type. We have found that an example of such a mixture in a pulsed HCD is the He–Kr–Hg mixture, where Hg^{+*} ions are pumped by charge exchange from He_0^+ [reaction (1a)] and Kr^{+*} ions are excited by transfer from He_m [reaction (1c)]. In this case He_0^+ ions do not undergo decay as a result of collisions with Kr_0 ions because of the significant difference in their level energies [$\Delta E(\infty) \gg kT$]; as a result, one can maintain a higher total pressure of working materials. The specific peak power in the He–Kr–Hg laser at the 615.0- and 794.5-nm Hg II lines and 469.4-nm Kr II line reached 0.25 W cm^{-3} in the repetitively pulsed regime. By varying the mercury-vapour pressure in a tube of volume $V = 40$ cm^3 (Fig. 5) it is possible to implement three lasing regimes: lasing at the blue Kr II line at $P(\mathrm{Hg}) = 0$; lasing at the red Hg II lines at $P(\mathrm{Hg}) = 10.7$ Pa (with an average power of about 8 mW kHz^{-1} at $f \leqslant 10$ kHz); and joint lasing at all lines, including the regime with equal powers at the blue Kr II and red Hg II lines (about 4 mW kHz^{-1}), at $P(\mathrm{Hg}) = 4.7$ Pa.

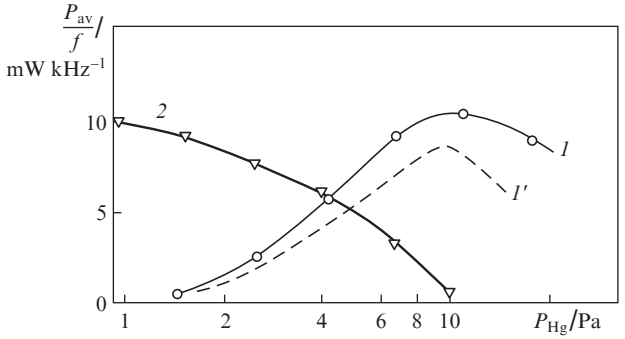

Figure 5. Dependences of the lasing power at the (*1*) 615-nm Hg II and 469.4-nm Kr II lines on the mercury vapour pressure in a pulsed HCD He–Kr–Hg laser at $P_{He} = 2.5$ kPa, $P_{Kr} = 5$ Pa, and $j = 0.9$ A cm^{-2} (experiment). Curve (*1'*) is the result of calculation for the 615-nm Hg II line at a conditional presence of charge exchange in the He–Kr mixture with a typical constant of $K'_{CE} = 10^{-9}$ cm^3 s^{-1} (gain in power is pronounced in the absence of charge exchange).

7. Conclusions

Pumping of HCD ion lasers by microsecond current pulses made it possible to increase significantly (in comparison with the cw and quasi-cw regimes) the gain and output power for lasing both at individual lines and in the multi-wavelength regime. The operating capacity of the active elements of these lasers in the repetitively pulsed regime with a pulse repetition rate up to 100 kHz was demonstrated. The optimal pulse repetition rates f were found and it was shown that the average power of radiation from active elements of relatively small size can be several tenths of watt and approach 1 W for cathodes 2 cm in diameter and more than 40 cm in length. We hope that the lasing power can be increased to few watts with a corresponding increase in the active-medium (i.e., the cathode cavity) volume, which, along with a high pulse repetition rate, will contribute to new applications of these lasers for data processing, medical and biological studies, etc.

References

1. Ivanov I.G., Sem M.F. *Proc. SPIE Int. Soc. Opt. Eng.*, **3403**, 120 (1998).

2. Little C.E. *Metal Vapour Lasers. Physics, Engineering and Application* (Chichester–New York–Brisbane–Toronto–Singapure: John Wiley & Sons, 1999).
3. Zinchenko S.P., Ivanov I.G., Sem M.F. *Proc. SPIE Int. Soc. Opt. Eng.*, **2110**, 150 (1993).
4. Ivanov I.G., Sem M.F. *Opt. Atmos. Okeana*, **14**, 1016 (2001).
5. Kravchenko A.V., Ivanov I.G. *Opt. Atmos. Okeana*, **22**, 1060 (2009).
6. Kalinchenko G.A. *Proc. SPIE Int. Soc. Opt. Eng.*, **4243**, 21 (2001).
7. Yakovlenko S.I. *Kvantovaya Elektron.*, **30**, 501 (2000) [*Quantum Electron.*, **30**, 501 (2000)].
8. Zinchenko C.P., Ivanov I.G. *Sb. tezisov dokladov XV Vserossiiskogo simpoziuma "Lazery na parakh metallov" (LPM-2004)* [Proc. XV All-Russia Symposium "Metal-Vapour Lasers" (MVL-2004)] (Rostov-on-Don: Diapazon, 2004) p. 20.
9. Piper J.A., Webb C.E. *Opt. Commun.*, **13**, 122 (1975).
10. Leigt B., Tobin R.C., Rozsa K., Donko Z. *J. Phys. D: Appl. Phys.*, **30**, 2946 (1997).